

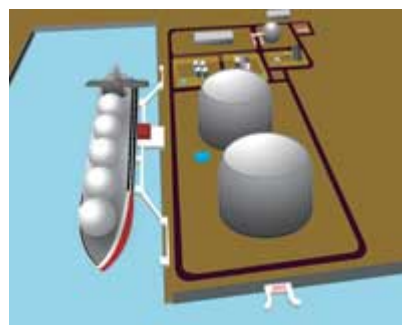


LNG Properties and Hazards

Understand LNG Rapid Phase Transitions (RPT)

An ioMosaic Corporation
Whitepaper

G. A. MELHEM, PH.D.
S. SARAF, PH.D.
H. OZOG



ioMosaic Salem

Corporate Headquarters
93 Stiles Road
Salem, NH 03079

Tel: 603-893-7009
Fax: 603-251-8384

ioMosaic Houston

2401 Fountain View Drive
Suite 850
Houston, TX 77057

Tel: 713-490-5220
Fax: 832-533-7283

ioMosaic Minneapolis

401 North 3rd Street
Suite 410
Minneapolis, Minnesota 55401

Tel: 612-338-1669
Fax: 832-533-7283

Copyright © 2006 ioMosaic Corporation. All rights reserved.

This document contains proprietary business information and may not be copied or distributed in any form without the express permission of ioMosaic Corporation.



Understand LNG Rapid Phase Transitions (RPT)

G. A. Melhem, Ph.D., ioMosaic Corporation, Salem, New Hampshire

H. Ozog, ioMosaic Corporation, Salem, New Hampshire

S. Saraf, Ph.D.

Abstract

The growing public concern over potential terror threats to LNG carriers and the expected increase in LNG shipping traffic led to several recent LNG safety studies^{1,2,3}. All of these studies addressed the consequences of LNG spills on water; however, none of these recent reports satisfactorily addressed the LNG rapid phase transition phenomenon.

Although rapid phase transitions are well researched, the literature published so far does not explicitly quantify the RPT phenomenon. The objective of this paper is to provide a clear understanding of how rapid phase transitions develop and how overpressure is generated.

We present a thermodynamic treatment of rapid phase transitions and discuss the estimation of hazard potential based on the superheat limit. ioMosaic's SuperChems Expert software is used to model multi-component LNG spills and to illustrate how LNG composition influences the development of rapid phase transitions and overpressure generation.

Introduction

A rapid phase transition is the very rapid (near spontaneous) generation of vapor as the cold LNG is vaporized from heat gained from the underlying spill surface or from large volumes of water contacting LNG in a storage tank. Because the vapor is evolved very rapidly, localized overpressure is created. This is also sometimes described as a physical explosion.

Following a release of liquefied natural gas (LNG) from a ship or storage tank, a liquid pool forms and spreads on the surrounding spill surface. Rapid phase transitions have been shown to occur during or following an LNG spill. The hazard potential of rapid phase

¹. ABS Consulting report for FERC, "Consequence Assessment Methods for Incidents Involving Releases from Liquefied Natural Gas Carriers", FERC04C40196, May, 2004.

². R. M. Pitblado, J. Baik, G.J. Hughes, C. Ferro, and S. J. Shaw, "Consequences of LNG marine incidents", Center for Chemical Process Safety (CCPS) Conference, Orlando, June 29 – July 1, 2004.

³. M. Hightower, L. Gritzo, A. Luketa-Hanlin, J. Covan, S. Tieszen, G. Wellman, M. Irwin, M. Kaneshige, B. Melof, C. Morrow, and D. Ragland, "Guidance on Risk Analysis and Safety Implications of a Large Liquefied Natural Gas (LNG) Spill Over Water", A Report Prepared by Sandia National Laboratories (SNL) for the U.S. Department of Energy (DOE), SAND2004-6258, Dec. 2004.



transitions can be severe, but is highly localized within or in the immediate vicinity of the spill area.

Rapid phase transitions are especially a concern for LNG ships because (a) the pressure rating of the actual LNG cargo tanks is low, and (b) the LNG cargo tanks pressure relief system may not be able to actuate quickly enough to relieve the large volumes of vapor that can be spontaneously generated by an LNG rapid phase transition⁴. Three scenarios of interest are addressed in this paper:

1. An LNG spill on water from the LNG ship cargo tanks from a large hole above the water line causing a rapid phase transition near the outer hull of the ship close to the release point.
2. An LNG spill into the water from the LNG ship cargo tanks from a large hole below the water line causing a rapid phase transition near the outer hull of the ship at the release point.
3. Water inflow into a partially full LNG cargo tank such that the large hole is below the water line but above the LNG liquid level in the LNG cargo tank.

RPT Scenarios of Concern for LNG Ships

A large hole in an LNG tanker storage vessel can be caused by a collision of the LNG tanker with another ship, grounding of the LNG tanker, and/or intentional acts of sabotage or terrorism. The location of the hole with respect to the water line, the initial LNG liquid level in the tanks, and the depth of the ship will influence the rapid phase transition outcome.

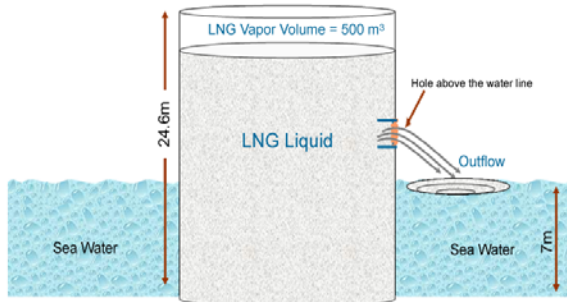
Hole above the Water Line:

In this case the LNG tank is near full, say 98 %, and breach occurs above the water line causing LNG to be released from the tank onto the water surface (see Figure 1). Rapid phase transitions will occur near the release point with potential damage to the outer ship hull, but not the tank. A liquid pool will form adjacent to the tanker. The extent of the hazard footprint and possible escalation events will depend on whether the LNG vapors ignition is immediate or delayed.

⁴ This assumes that the tanks are not first damaged by the high levels of overpressure created by the rapid phase transition itself.



Figure 1: LNG Outflow from a Hole Above the Water Line

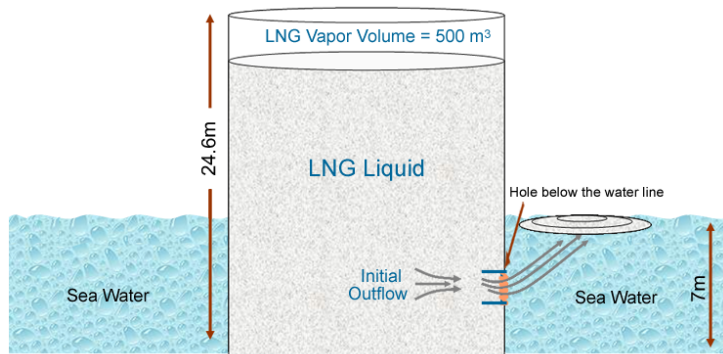


Source: ioMosaic Corporation

Hole below the Water Line:

In this case the LNG tank is near full, say 98 %, and breach occurs below the water line causing LNG to be released initially from the tank into the surrounding water medium (see Figure 2). The initial flow rate is driven by the LNG liquid head which is larger than the liquid head of the surrounding water. Rapid phase transitions will occur near the release point with potential damage to the outer ship hull, but not the tank. This mode of release will continue until the pressure inside the LNG tank equilibrated with the pressure exerted by the surrounding water. At this point, gravity flow will cause water to intrude into the LNG tank and LNG to flow out. It is likely that this type of flow will lead to small rapid phase transitions that can cause damage to the outer hull of the ship but not the tank.

Figure 2: LNG Outflow from a Hole below the Water Line



Source: ioMosaic Corporation



Table 1: Hole below the Water Line Typical Scenario Data

Release Variable	Moss spherical vessel	Membrane vessel
Single tank capacity	27,450 m ³	27,450 m ³
Tank dimensions	37.5 m inner diameter	W=34.5m, L=32m, H=24.6m
Typical vessel draft	11.5 m	11.5 m
Bottom of tank below the waterline	9.5 m	7 m
Initial LNG hydrostatic head	33.8 m	23.6 m
Water backpressure head	0.87 barg	0.63 barg
Assumed initial water entry to create 0.2 barg pressure	90 kg	90 kg
Pressure differential between LNG at hole to seawater at hole	0.71 barg	0.54 barg
Initial LNG discharge rate	2100 kg/s (0.75 m hole) 8300 kg/s (1.5 m hole)	1800 kg/s (0.75 m hole) 7200 kg/s (1.5 m hole)
Initial LNG discharge velocity	11.1 m/s	9.6 m/s
Equilibrium point (% of tank level)	43 %	43 %

Any LNG vapor generated as the water intrudes into the LNG storage tank will create higher pressure on the LNG side and will cause the water intrusion to stop. It is possible for this meta-stable equilibrium state to continue for a very long time.

This scenario has also been addressed by two recent papers by Shaw⁵ and Fay⁶. The example presented by Shaw is summarized in Table 1. Note that tank is initially 98 % full with 500 m³ of vapor space and that the hole considered is 0.5 meters above the bottom of the tank. A small amount of water is required to raise the pressure inside the tank by 0.2 barg.

Hole Below the Water Line but Above LNG Liquid Level:

In this case the LNG tank is partially full, say 25 %, and breach occurs below the water line but above the LNG liquid level (see Figure 3). If the hole size is sufficiently large, say 5 meters in diameter, it is possible for enough water to enter the LNG tank and mix with the cold LNG at the LNG surface causing an RPT inside the tank. As the water mixes with the LNG it gives up its sensible heat as liquid until it freezes, it then gives up its heat of fusion, and finally its sensible heat as solid as its temperature drops from 273.15 K to the boiling point of LNG, 111 K.

The RPT localized overpressure can be as high as 36 bars as shown later in this paper and can cause severe damage to the tank walls. In addition, the near instantaneous vapor generation⁷ from one second of water flow from a 5 meter hole into a typical LNG tank that

⁵ Shaw et al, "Consequences of underwater releases of LNG", AIChE Spring Meeting, Atlanta, GA, April 10 – 14, 2004.

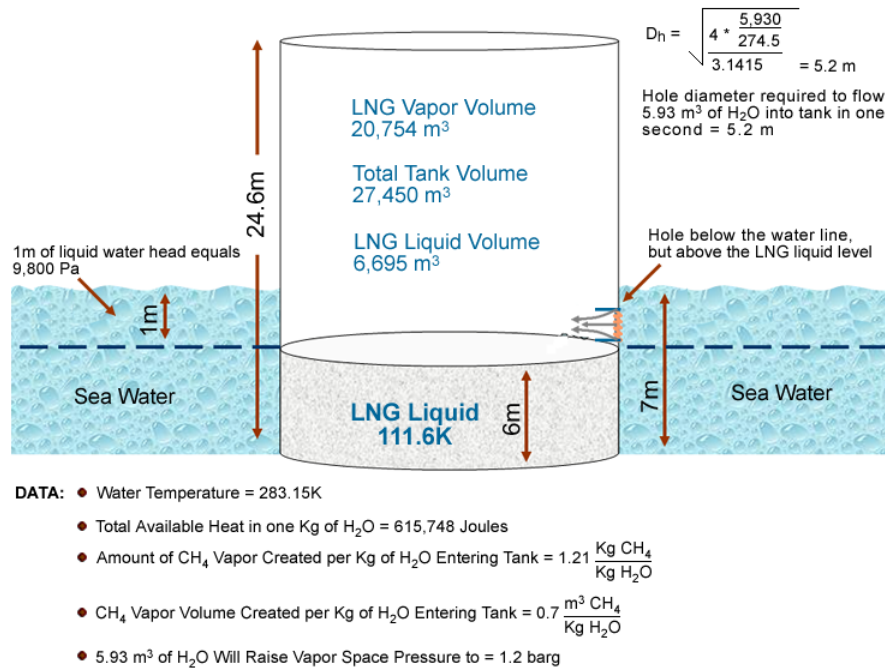
⁶ Fay, "Model of spills and fires from LNG and oil tankers", JHM, B96, 2003, 171 – 188

⁷ Assumes that the water gives up its heat content very rapidly



is 25 % full can raise the vapor space pressure to the design limit of the tank. In order to stop water ingress into the tank, the pressure in the vapor space of the tank has to be equal or greater than the pressure imposed by the difference between the water and LNG liquid levels.

Figure 3: Hole below the Water Line but above LNG Liquid Level



Source: ioMosaic Corporation

Although one can show this hypothetical scenario where the integrity of one or more of the LNG storage tanks may be at risk from a RPT or the rapid vapor generation associated with a RPT, we must keep in mind that this particular scenario requires the tanks to be partially empty. If the fill level is low enough, the potential fire and flammable dispersion impact zones may be smaller than other scenarios considered where the tanks are near full.

Prediction of RPT Hazard Potential

Rapid phase transitions are also referred to as physical explosions. This type of explosion does not involve combustion or a chemical reaction to create mechanical explosion energy. Instead, mechanical or explosion energy is created from the rapid expansion of a high pressure meta-stable fluid to ambient pressure.

A fluid can be made thermodynamically unstable (meta-stable) by rapidly changing its temperature and pressure such that it cannot exist at those conditions in its initial state (all liquid).

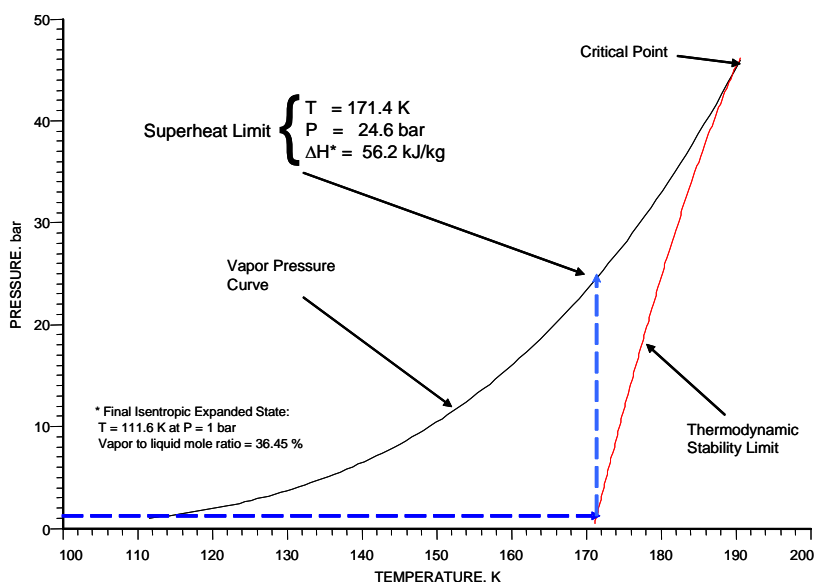


Even during very rapid heating or very rapid depressurization, all fluids must change phase ultimately. These phase change limits (also called the thermodynamic stability limits) can be determined accurately using an equation of state. An LNG rapid phase transition can be explained using the thermodynamic stability limit (also called the superheat limit).

We illustrate the rapid heating process of LNG leading to a rapid phase transition on a phase diagram. LNG consists predominantly of methane. Certain LNG compositions will contain higher fractions of ethane and some propane and as a result their phase diagram is different from that of pure methane.

First let's look at how the superheat limit is reached for pure liquid methane. This is illustrated graphically in Figure 4.

Figure 4: The Superheat Limit for Pure Methane



Source: SuperChems Expert v5.7, ioMosaic Corp.

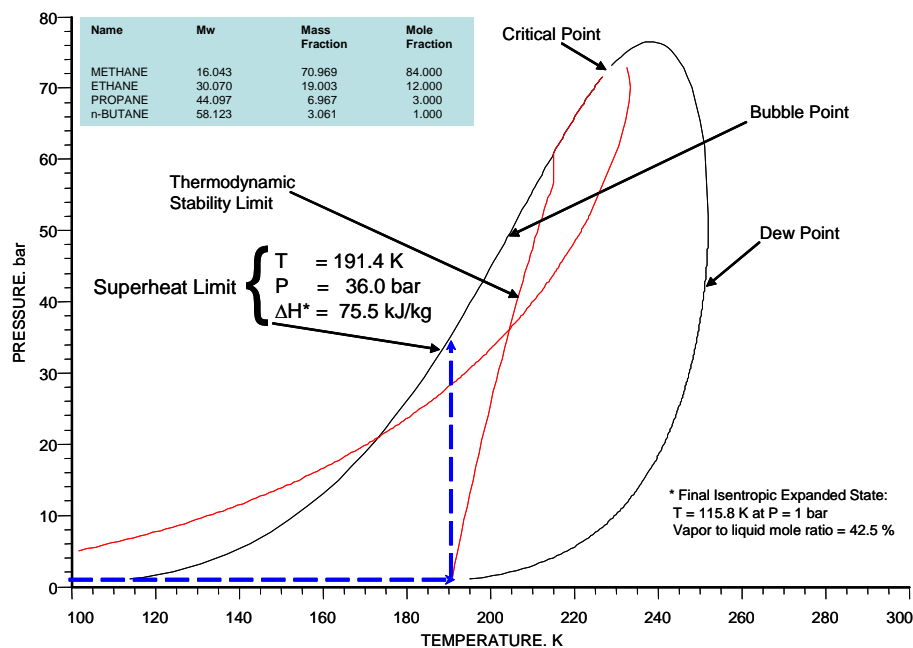
Follow the dashed blue line at the bottom of Figure 4. Pure liquid methane boils at 111.6 K (-258.8 F) at ambient pressure. Rapid heating at ambient pressure causes methane to reach the thermodynamic stability limit of 171.4 K (-151.15 F). Once heated to that temperature, methane becomes a superheated liquid, i.e. a saturated liquid with a vapor pressure of 24.6 bars. Methane reaches the superheated state and has to give up its superheat by expanding because the ambient pressure is 1 bar. If we assume that the expansion process is reversible/isentropic (we can bring methane back to its superheated state by adding back the same amount of energy it lost when it expanded) methane will expand to 1 bar and exert 56.2 kJ/kg in mechanical work (physical or pressure-volume) or energy (on the surroundings) that can be used to create overpressure, i.e. explosion energy.



In reality, the expansion process is not reversible and its efficiency at best is around 50 % as established by actual testing⁸. This is because the expansion process loses energy as it creates turbulence and as the liquid flashes to vapor. As a result, the maximum possible rapid phase pressure that methane can reach is 24.6 bars and its mechanical explosion energy is 28.1 kJ/kg. This is equivalent to burning 0.56 grams of methane vapor. In other words, on per unit mass basis, the methane combustion process produces 1,780 times more energy than a rapid phase transition. This is why, historically, rapid phase transition overpressure estimates were excluded from LNG risk assessments and considered to be negligible and localized.

Now let's repeat the same process for an LNG mixture. An LNG mixture containing high fractions of ethane and propane is more likely to undergo a rapid phase transition than pure methane. This is observed in real LNG spills and can also be proven theoretically as illustrated in later sections of this paper.

Figure 5: The Superheat Limit for an LNG Mixture



Source: SuperChems Expert v5.7, ioMosaic Corp.

Instead of a vapor pressure curve, an LNG mixture has a phase envelope consisting of a bubble point curve and a dew point curve as illustrated in Figure 5.

Follow the dashed blue line at the bottom of Figure 5. This LNG mixture boils at 115.8 K at ambient pressure. Rapid heating at ambient pressure causes the LNG mixture to reach

⁸ G. A. Melhem, "Advanced Consequence Analysis", Arthur D. Little Inc., 1998.



the thermodynamic stability limit of 191.4 K. Once heated to that temperature the LNG mixture becomes a superheated liquid, i.e. a saturated liquid with a bubble point pressure of 36.0 bars. The LNG mixture reaches the superheated state and has to give up its superheat by expanding because the ambient pressure is 1 bar. If we assume that the expansion process is reversible/isentropic, the LNG mixture will expand to 1 bar and exerts 75.5 kJ/kg in mechanical work or energy that can be used to create overpressure, i.e. explosion energy.

As mentioned earlier, the expansion process is not reversible and its efficiency at best is around 50 %. As a result, the maximum possible rapid phase pressure that the LNG mixture can reach is 36.0 bars and its mechanical explosion energy is 37.75 kJ/kg. An LNG mixture rapid phase transition produces 1,325 times less overpressure energy per unit mass than the combustion process.

The explosion energy predicted by the superheat limit at 37.75 kJ/kg or (20.7 kJ/liter) is consistent with recent spill data measured by Shell⁹ at 5.6 kJ/liter. Until a more detailed model is developed to better represent the rapid phase transition process, we recommend the use of the superheat limit explosion yield of 20.7 kJ/liter. This number can easily be established for other LNG compositions of interest.

Although not recommended by this author, the explosion yield of 20.7 kJ/liter can be used with a simple TNT¹⁰ equivalency method to predict overpressure contours from a rapid phase transition with a specified amount of LNG. Note that TNT equivalence will over predict near field overpressure values and is therefore considered to be a conservative method.

Even if we were to consider the physically impossible, i.e., the entire contents of one LNG storage tank (say 25,000 m³) participated in a single RPT at the same time (only a small portion of the liquid spilled on water that is in intimate contact with the spill surface has been shown to participate in an RPT in large scale field trials), the overpressure hazard radius to 1.0 psi would be estimated at 0.82 miles from the center of the RPT. The RPT hazard radius is well within distances of concern of LNG flammable dispersion to ½ LFL for releases from hole sizes ranging from 1 to 5 meters.

Predicting RPTs from LNG Spills

Existing modeling methods fall short from being able to identify with accuracy what fraction of an LNG spill will participate in a rapid phase transition¹¹. However, there are

⁹ V. T. Nguyen, "Rapid Phase Transformations: Analysis of the large scale field trials at Lorient", Shell Research Limited, External Report TNER.86.058, February 1987.

¹⁰ TNT equivalence will over-estimate overpressure in the near field because the TNT charts are based on the use of a solid explosive and not a physical explosion (PV energy)

¹¹ F. Briscoe and G. J. Vaughn, "LNG/Water Vapour Explosions – Estimates of Pressures and Yields", UK AEA SRD R 131, October 1978.



advanced modeling techniques that can tell us if a rapid phase transition will occur and at what approximate time during the spill it will occur.

Before discussing RPT modeling, one needs to understand the different boiling regimes based on the temperature difference between the heating medium and the cold liquid. Figure 6 illustrates the various boiling regimes for methane and nitrogen.

The process of forming vapor in all liquids (also referred to as flashing) usually involves what is called nucleation sites. For example, in a process vessel, these nucleation sites can be small imperfections on the vessel inner surface or tiny colloidal suspensions of dirt or dissolved gas in the liquid. Nucleation is a process where vapor bubbles start to form in these surface imperfections when a liquid is heated to a boiling state. The nucleation process requires mass and heat transfer in order to produce vapor. If heating occurs at an extremely rapid rate, these nucleation sites are rendered inactive as they do not have enough time to complete the mass and energy transfer/exchange required to generate the vapor bubbles, i.e. nucleate. The same effect can be produced by dropping the pressure of a saturated fluid very fast.

When LNG is spilled on land or water, LNG is initially very cold (110 K or -261.67 ° F). The spill surface (land or water) is initially very hot compared to the temperature of LNG. Even cold ocean water is typically around 60 ° F or 289 K. The initial difference between the LNG and the water surface is 289-110 or 179 K (322 ° F). This high temperature difference causes the LNG to start boiling. Because the difference in temperature is so high initially, a vapor film is formed at the contact point between the LNG and the underlying spill surface (see Figure 3).

This vapor film will persist until the spill surface cools enough and/or until the LNG bubble point temperature gets high enough as methane is preferentially depleted from the liquid LNG spill. As long as the vapor film exists between the LNG and the spill surface, heat transfer is greatly reduced (vapor layer acts as an insulator also). When the difference in temperature between the LNG and the spill surface gets smaller, the vapor film is destroyed and a different (faster) heat transfer mode begins (see Figure 3). The rate of heat exchange between the cold LNG and the warmer spill surface is now orders of magnitude larger than it was with the vapor film intact. As a result, the LNG is heated very rapidly (almost instantaneously to the superheat limit) and a rapid phase transition occurs.



Figure 6: Boiling Regimes for Methane and Nitrogen

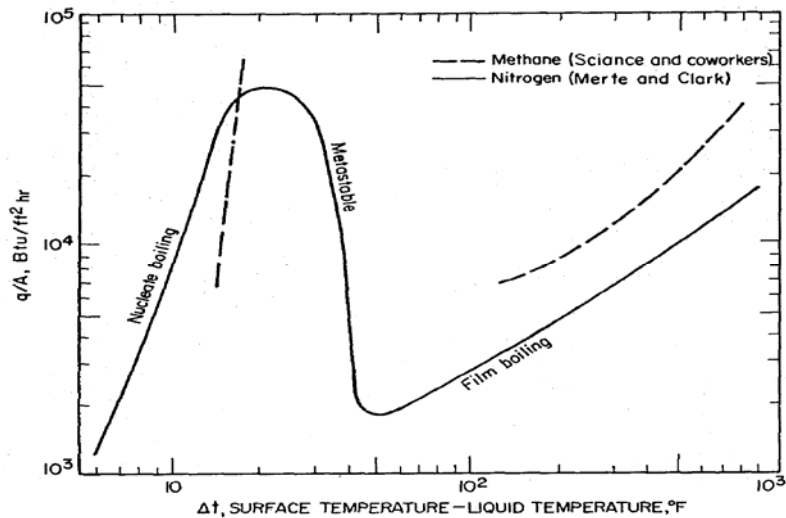
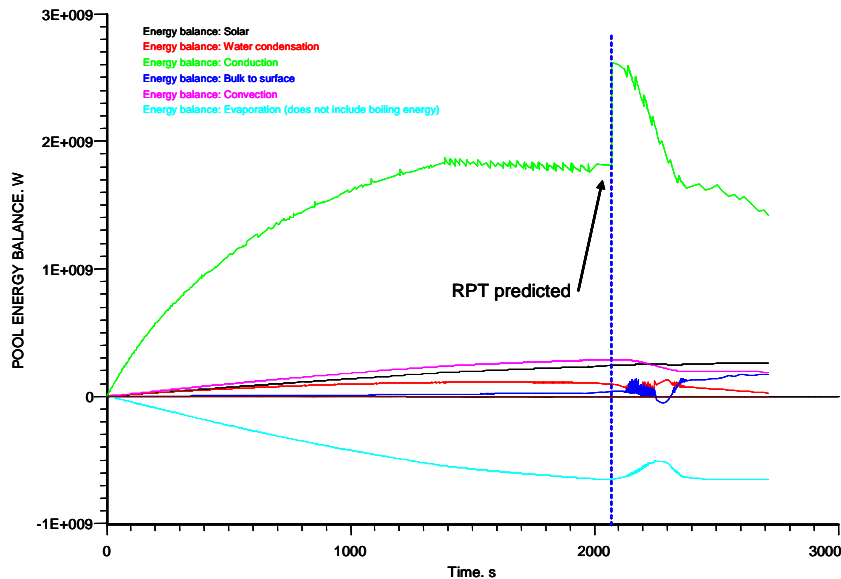


Figure 7: Detailed liquid pool energy balance for an LNG mixture spilled on water



Source: SuperChems Expert v5.7, ioMosaic Corp.

We illustrate this advanced modeling methodology using an example. We contrast a large liquid spill of LNG consisting of pure methane to that of an LNG mixture containing high fractions of ethane and propane. The liquid spill occurs over 33 minutes at a rate of 5,300 kg/s (equivalent to spilling the entire contents of a 25,000 m³ LNG sphere from a 1 m hole) on water with a water initial temperature of 295 K at an atmospheric stability class F and a

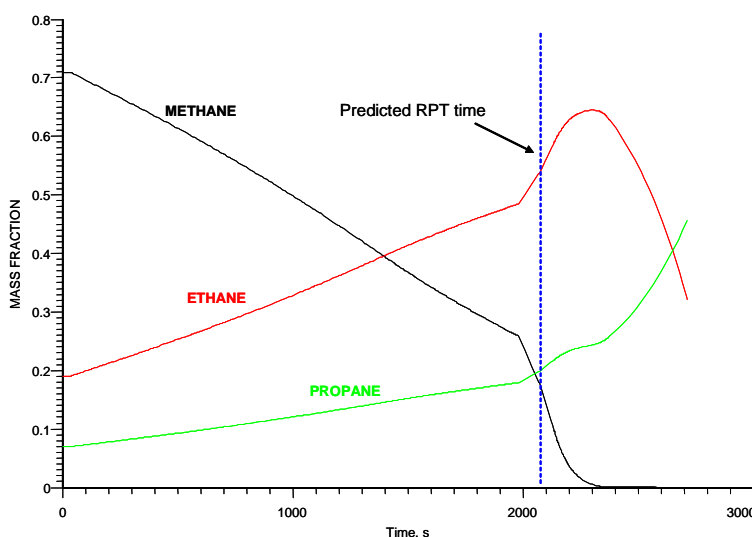


10 m wind speed of 2 m/s. Details of the pool spreading and vaporization model are available in one of our recent publications¹².

This liquid pool simulation was generated using SuperChems Expert. The pool spreading is calculated based on a differential solution of the Shallow water equations. SuperChems considers in detail the different liquid spreading regimes and the pool energy balance. The spilled liquid is divided into a bulk liquid phase and a small liquid phase at the surface/interface. Heat transfer between the spilled liquid and the spill surface occurs as a function of time, depth, and radial position. This particular simulation shows that a rapid phase transition will occur at approximately 2,080 seconds (shortly after the spill ends) as evidenced by the increased rate of conductive heat transfer caused by the transition from film to pool boiling (see Figure 4).

As shown by Figure 8, the rapid phase transition coincides with decreasing methane concentrations in the liquid pool. As the pool spreads and exchanges heat with the spill surface, methane is preferentially boiled off, leading to higher concentrations of ethane and propane. This theoretical finding is supported by actual spill field tests (see Appendix A).

Figure 8: LNG pool mixture composition



Source: SuperChems Expert v5.7, ioMosaic Corp.

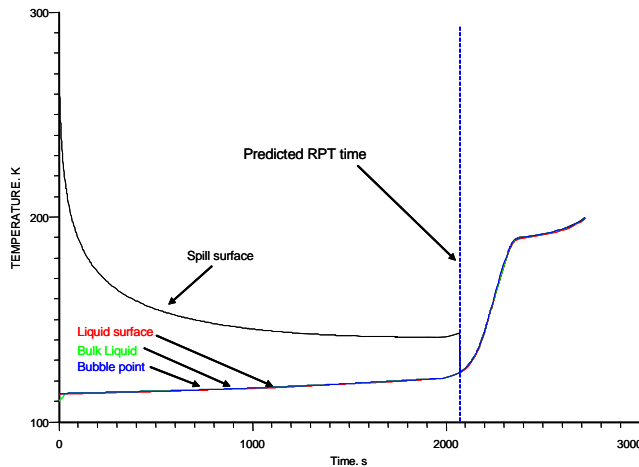
The rapid phase transition occurs when the bulk methane composition in the pool is less than 20 % by weight and the ethane fraction is more than 50 % by weight. As ethane, propane, and butane fractions in the pool increase, the mixture boiling point becomes much higher than that of pure methane. This is illustrated in Figure 9. Note that the bulk liquid temperature, bubble point, and pool surface/interface temperature as essentially the same

¹² S. R. Saraf and G. A. Melhem, "Modeling LNG Pool Spreading and Vaporization", AIChE Spring Meeting, Atlanta, GA, April 10 – 14, 2005.



since the liquid is at its boiling point the entire time. The spill surface temperature decreases with time as the interface cools and the bubble point of the mixture increases as methane is depleted preferentially from the pool. As the temperature difference between the surface and LNG reduces, the boiling regime changes from film boiling to nucleate boiling resulting in higher heat transfer rates.

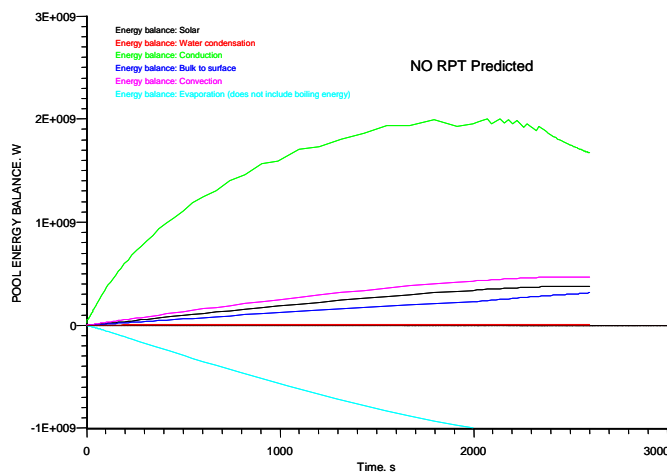
Figure 9: Predicted LNG mixture and pool surface interface temperatures



Source: SuperChems Expert v5.7, ioMosaic Corp.

A rapid phase transition is not predicted for the same spill consisting of pure methane as illustrated in Figure 10. In this example because the critical temperature difference to transit from film boiling to nucleate/pool boiling is not reached. As shown by the Shell data in Appendix A for methane, when the substrate temperature is low boiling or cold, ice formation is observed. The behavior turns violent as the substrate temperature increases.

Figure 10: Detailed energy balance for a pure methane spill on water



Source: SuperChems Expert v5.7, ioMosaic Corporation



Conclusions

We have surveyed the open literature about LNG rapid phase transitions. Data summaries and details can be found in Appendix A. Several conclusions and insights can be obtained from the published data:

1. Rapid phase transitions were observed in many but not all field trials.
2. Rapid phase transitions are more likely to occur in LNG mixtures containing very high fractions of ethane and propane. LNG composition is a critical parameter.
3. Spill rate, spill duration, and the spill surface conditions influence the rapid phase transition process. Higher spill rates and longer spill durations are more likely to produce rapid phase transitions. Critical temperature difference leading to nucleate/pool boiling heat transfer is more likely to be reached if more cold liquid is spilled or if cold liquid is spilled over a long duration.
4. Only a small fraction of the spilled LNG was observed to undergo rapid phase transitions.
5. The superheat limit theory for rapid phase transition provides an upper bound on the explosion yield that can be used in risk assessments and safe separation distance studies.

The explosion energy predicted by the superheat limit at 37.75 kJ/kg or (20.7 kJ/liter) is consistent with recent spill data measured by Shell¹³ at 5.6 kJ/liter. Until a more detailed model is developed to better represent the rapid phase transition process, we recommend the use of the superheat limit explosion yield of 20.7 kJ/liter. This number can easily be established for a wide range of LNG compositions of interest.

The hazard potential of rapid phase transitions can be severe, but is highly localized within the spill area.

¹³ V. T. Nguyen, "Rapid Phase Transformations: Analysis of the large scale field trials at Lorient", Shell Research Limited, External Report TNER.86.058, February 1987.



Appendix A: RPT Test Data Summaries

Nakanishi and Reid¹

Test Setup

A variety of spills were performed in a 200 ml. Dewar flask at the MIT laboratory in 1971.

Test Condition

Component	Condensed pipeline gas (CPG)	Liquefied methane gas (LMG)	Liquefied ethane gas (LEG)	Synthetic liquefied natural gas (SLNG)
	wt %			
Methane	92.7	100	-	80 – 90
Ethane	Trace	-	100	-
Propane	0.0	-	-	20 – 10
Nitrogen	7.3	-	-	0 – 2



Test Data

Test series	Spilled liquid	Volume (μm3)	T (° C)	Substrate	Substrate volume (μm3)	Substrate T (° C)	Observation
A	Water			CPG			Freezing of water droplets; popping sound reported when the drops were exposed to air or water
A				LN2			Freezing of water droplets
B	Water	200	5	CPG or LMG or LEG or LN2	200		No explosion
C	CPG or LMG or LEG	1 – 5		Water		5 – 10	Ice formation
	CPG or LMG or LEG	1 – 5		Water		80	Ice formation; ice fragments foamed up and popped
C	LN2			Water		5 – 10	Ice formation
C	LN2			Water		80	Ice formation
E	CPG			Ice		- 150	Foaming and gas bubbles
E	LN2			Ice		- 150	Foaming and gas bubbles
E	CPG			Ice		- 5	Foaming and gas bubbles
E	LN2			Ice		- 5	Gas bubbles
F	CPG			3 wt % NaCl in water		15	Ice formation
F	LN2			3 wt % NaCl in water		15	Ice formation
F	CPG			20 wt% ethylene glycol in water		15	Ice formation; ice fragments foamed up and popped
F	LN2			20 wt% ethylene glycol in water		15	Ice formation



Test series	Spilled liquid	Volume (μm3)	T (° C)	Substrate	Substrate volume (μm3)	Substrate T (° C)	Observation
G	LN2			ethylene glycol or cyclohexane or n-butyl alcohol			Ice formation
G	CPG or LMG or LEG	50 - 100		ethylene glycol or cyclohexane or n-butyl alcohol			Eruption reported
G	LN2			n-hexane or n-pentane or methyl cyclohexane			Ice formation
	CPG	< 10		n-hexane			Ice formation; ice fragments foamed up and popped
G	CPG, SLNG	10 - 100		n-hexane or n-pentane or methyl cyclohexane			Explosion
H	CPG, LMG, LEG, or	50		1 mm n-hexane film on water ¹			Explosion
H	CPG			Mercury or mercury coated with ethylene glycol or n-butyl alcohol			Rapid evaporation
H	CPG			Mercury coated with n-hexane or n-pentane or n-butane or methylcyclohexane			Explosion
H	CPG			Mercury coated with water or cyclohexane			No explosion
H	CPG			Benzene film on water			No explosion
H	CPG			Toluene film on water			Explosion
H	CPG			p-xylene film on water			No explosion
H	SLNG			Water coated with pentane or gasoline			Explosion

Notes: 1. No explosion noted if the film was frozen

2. LN2 – liquefied nitrogen

The authors propose that if the substrate is chemically “similar” to the cryogen spilled and the interfacial liquid has a low freezing point, then an explosion may occur.



Bureau of Mines²

Test Setup

The U.S. Bureau of Mines conducted LNG spills onto water in strip mine lane near Florence, PA.

Spill dimensions

The lake was approximately 67 m wide at the midpoint.

Instrumentation and data acquisition system

N/A.

Test Conditions

LNG composition

Series 1:

Storage duration	Methane	Ethane	Propane	Butane	Pentane	Ethane Plus Heavies
	mol %					
First week (avg.)	86.9	11.3	1.3	0.4	0.06	11.8
Second week (avg.)	87.8	10.6	1.2	0.3	0.06	11.0
Third week (avg.)	85.6	12.7	1.3	0.3	0.05	13.1
Fourth week (avg.)	81.3	16.5	1.7	0.4	0.06	17.0
Fifth week (avg.)	77.4	20.1	2.0	0.4	0.07	20.6
36 th day	72.2	24.6	2.5	0.6	0.07	25.3
37 th day	51.5	41.5	5.6	1.2	0.19	42.9
38 th day	55.2	38.7	4.9	1.0	0.14	39.8
42 nd day	0.5	67.6	25.8	5.3	0.82	73.7



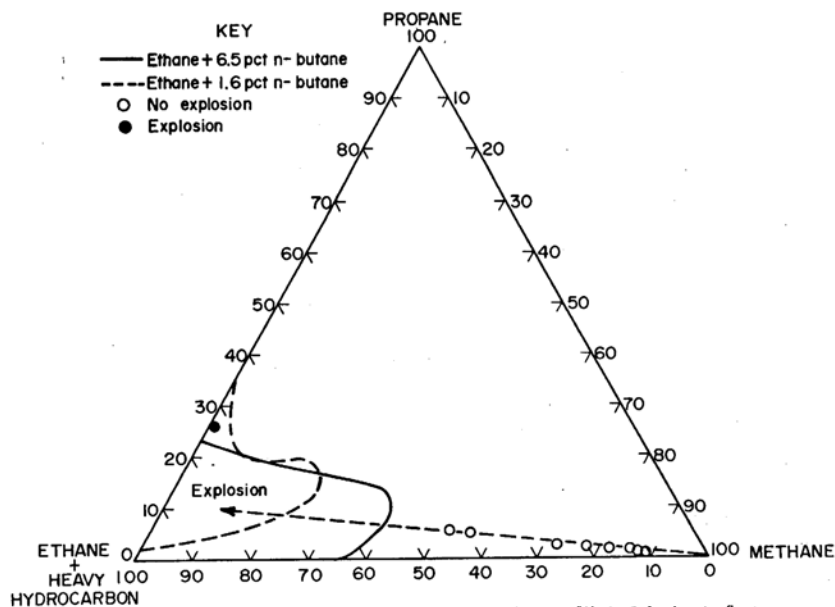
Series 2:

Date	Methane	Ethane	Propane	Butane	Pentane
(1971)	mol %				
12 th Oct.	88.8	9.2	0.81	0.15	0.03
19 th Oct.	78.3	19.5	1.8	0.34	0.06
21 st Oct.	56.2	39.7	3.3	0.66	0.16

Test Data

Series 1: Through the 39th day of evaporation when 0.038 m³ (10 gallons) of LNG remained in the tank the methane concentration was about 50%, the weathered LNG gave nothing more than crackling noise. On the 42nd day when 0.01 m³ (2.5 gallons) of LNG remained, the weathered LNG gave an immediate, violent explosion on water. Based on the observations a vapor explosion – composition diagram was proposed (Figure 11). The

Figure 11: Aging curve for LNG and vapor-explosion behavior²



solid curve of the figure encloses explosive concentrations of weathered LNG when the n-butane mole fraction of LNG is 6.5 % of the ethane mole fraction. The dashed curve encloses a smaller explosive zone when there is less n-butane in the LNG.

Series 2: About 7.6 m³ (2000 gallons) of Series 2 weathered LNG (low concentrations of butane and higher heavies) was released on water in three tests without any audible explosions.



UMCP³

Small-scale tests were performed with methane-rich LNG spilled onto water, pure organic liquids, and water-organic mixtures.

Test Setup

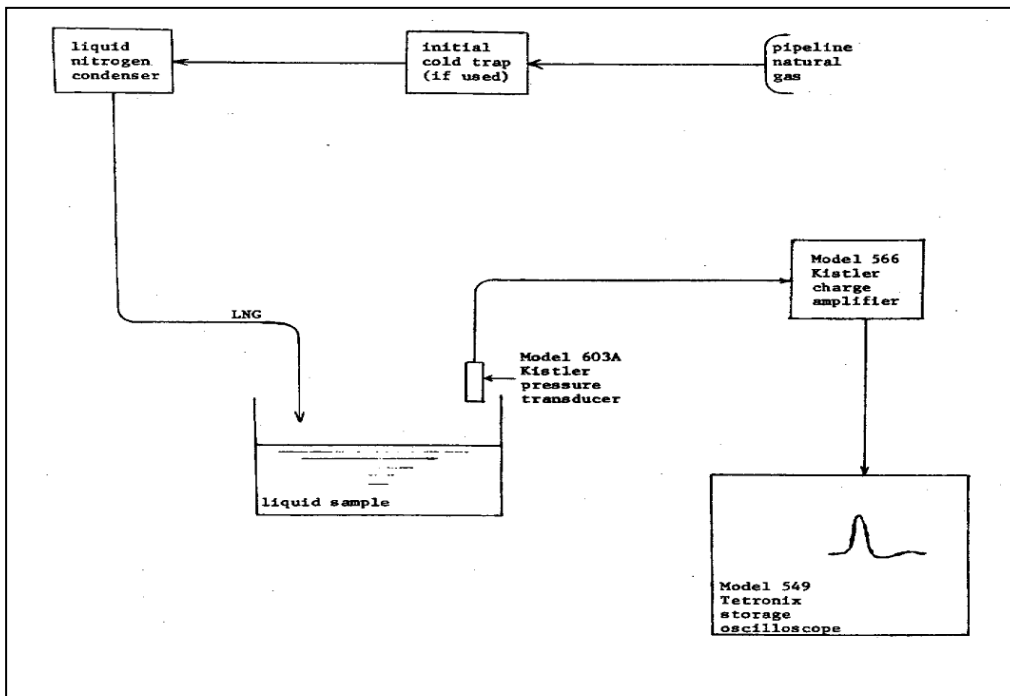
Spill dimensions

5 – 200 μm^3 (5 – 200 ml) of LNG was spilled.

Instrumentation and data acquisition system

The experimental setup is shown in Figure 12. Temperature or pressure was followed by the appropriate measuring device and displayed on an oscilloscope.

Figure 12: UMCP RPT studies³





Test Conditions

LNG composition

Component	%
Methane	95.1
Ethane	3.0
Propane	0.8
Butane	0.3
Pentane (all isomers)	0.1
Carbon dioxide	0.7
Nitrogen	0.01

Test Data

Test series	LNG volume	Substrate	Substrate volume	Result
	μm^3		μm^3	
A-1				
	5 – 20	Distilled water	40	No RPT
		Distilled water with 8.8 wt % NaCl	40	No RPT
		Distilled water saturated with CO ₂	40	No RPT
A-2				
		Toluene, methanol mixture	40	No RPT
		Toluene, methanol, water mixture	40	No RPT
		Toluene, s-butyl alcohol, water mixture	40	No RPT
		Chlorobenzene	40	No RPT
		n-hexane mixture	40	No RPT
		Water, chlorobenzene, toluene mixture	40	No RPT
		1-butanol	40	No RPT
		sec-butyl alcohol	40	No RPT
		n-hexane, water mixture	40	No RPT
		n-hexane, water, toluene mixture	40	No RPT
		Toluene, chloroform mixture	40	No RPT
		Methyl cyclohexane mixture	40	No RPT
A-3				
	45 – 55	Water	40	No RPT
B-1 ¹				
	10 – 100	1 mm hexane film on water	100	RPT reported
		1 mm toluene film on water	100	RPT reported



Test series	LNG volume	Substrate	Substrate volume	Result
	μm^3		μm^3	
	100 – 200	Hexane	-	RPT reported
B-2 ²				
	≥ 50	1 mm hexane film on water	-	RPT
	Up to 200	1 mm toluene film on water		No RPT
C-1				
	10 – 100	Hexane film on water	-	RPT
C-2 ³				
	150 – 200	Pure hexane	-	RPT
C-3 ⁴				
	100	Pure hexane	100	RPT

Notes: 1. Pipeline gas was passed through a -25°C cold trap before condensation.

2. Pipeline gas was passed through a dry ice/methanol cold trap (-78°C) and condensed in liquid nitrogen cold trap.

3. Observed ΔP_{max} varied with hexane volume.

Hexane	ΔP_{max}
μm^3	kPa
189	2836.4
122	2127.3
77	1823.4

4. Un-pretreated LNG was repeatedly dropped onto hexane.

The authors concluded that composition of LNG is important in noticing RPT behavior and that the presence of a hydrocarbon film on water increases the probability of RPT occurrences.



Shell⁴

Test Setup

A series of spill experiments involving hydrocarbons and hydrocarbon mixtures on ambient and hot water were performed at Shell to study the RPT phenomenon.

Test Conditions

N/A.

Test Data

Table 2: RPT data for hydrocarbons on water

Compound	Sp. Gr. at NBP	NBP	Water Temp., range tested	Results
		^o C	^o C	
Iso-butane	0.63	- 11.7	18 – 89	Boiling, no ice
			93 – 99	Vapor explosions
Freon 22	~ 1.2	- 40.8	41 – 43	Ice
			46 – 82	Vapor explosions
Propane	0.57	- 42.1	0 – 52	Ice
			53 – 70	Vapor explosions
			71 – 82	Rapid pops
Propylene	0.61	- 47.7	38 – 41	Ice
			42 – 75	Vapor explosions
			80 – 85	Rapid pops
Ethane	0.55	- 88.6	7 – 64	Ice forms, no pops
LNG (95 % methane)	0.43	- 161.5	0 – 32	Ice
			35 – 65	Disk boiling, pops
Nitrogen	0.81	-195.7	14 – 49	Ice forms, no pops

Note: RPTs are referred as vapor explosions

It has been reported that explosive boiling of LNG on ambient water can be produced when the methane content is less than 40 mol% along with a few mole percent n-butane.

Vapor explosion cannot occur with propane in excess of 20 mol %. Pure ethane did not produce a RPT on ambient water. Generally, small addition of heavier hydrocarbons increased the probability of RPT occurrence.



ESSO/API test⁵

Test Setup

A total of 17 spills were performed by ESSO Research and Engineering Company under contract with American Petroleum Institute (API) during Oct. 22 – Nov. 21, 1971.

Spill dimensions

0.95 – 9.5 m³ (250 – 2500 gallons) of LNG spills was discharged into Matagorda Bay in Texas at 18.9 m³/min (5000 gallons/min).

Instrumentation and data acquisition system

Downwind concentrations were monitored by hydrocarbon detectors at various elevations.

Test Conditions

LNG composition

Run no.	Spill size m ³	Methane ^a mol %	Spill duration sec.
1	0.78	85.2	-
2	0.73	85.8	5.6
3	0.84	85.3	5.8
4	0.93	88.0	5.2
5	0.93	87.6	-
6	0.79	87.4	-
7	0.79	87.4	7.0
8	7.12	85.1 ^b	25.0
9	7.42	88.8	25.0
10A	5.22	93.0	21.0
11	10.22	93.3	35.0
12	0.93	92.8	6.2
13	0.93	92.8	6.3
14	0.93	92.8	6.7
15	2.50	87.6	12.0
16	7.57	92.7	28.0
17	8.36	94.1	31.0

Notes: a. Runs 1 - 10A: % methane calculated from material balance data.

Runs 11 – 17: % methane calculated from samples obtained by capillary method.

b. Average composition calculated from a heel of 60% methane and fresh material of 94% methane.



Meteorological information

Run no.	Date (1971)	Wind speed m/s	Temp. °C	Rel. humidity %
1	Oct. 22	5.4	24	74
2	Oct. 22	5.4	24	74
3	Oct. 24	2.2 – 2.7	25	60-70
4	Oct. 26	9.4	26	79
5	Oct. 28	5.4	29	78
6	Oct. 28	4.9	29	79
7	Oct. 28	4.5	28	78
8	Nov. 1	4.9	29	78
9	Nov. 9	0 – 1.4	24	82
10	Nov. 11	2.2	20	54
11	Nov. 13	8.1	27	78
12	Nov. 14	8.0 – 8.5	25	75
13	Nov. 14	8.0 – 8.5	25	75
14	Nov. 14	6.7 – 7.6	25	72
15	Nov. 16	5.8	25	80
16	Nov. 20	0.0	18	62
17	Nov. 21	4.0	17 - 18	85-86

Notes: The water temperature was 22.2 – 23.3 °C

Test Data

“Explosions” occurred during test 8. LNG was poured onto water over a period of 25 seconds. Four explosions occurred in quick successions 42 second after the start (17 seconds after the end) of the spill period.



MIT LNG Research Center^{6,7}

Test Setup

Spills were made with six pure hydrocarbons (ethane, propane, iso-butane, n-butane, propylene, isobutylene) on water and other substances over a wide range of temperature. Five binary-hydrocarbon mixtures of ethane or ethylene with heavier hydrocarbons (propane, n-butane, n-pentane) were also studied.

Spill dimensions

Normally 0.0005 m^3 (500 cm^3) of hydrocarbons were spilled on a water area of 0.02 m^2 (200 cm^2 , $\sim 16 \text{ cm}$ diameter).

Instrumentation and data acquisition system

RPTs were monitored with a high frequency quartz pressure transducer located at the bottom of a polycarbonate hot-liquid container.

Test Conditions

LNG composition

N/A

Meteorological information

Laboratory experiments

Test Data

Pure alkanes and alkenes

Cryogen	Substrate	Substrate temperature K	Result Reproducibility ¹
Ethane	Water	278 – 313	Boiling, ice forms
Ethane	Ammonia – Water	271 – 297	Boiling, no ice forms
Ethane	Methanol	264 – 305	Eruptions
		306 – 331	Weak RPTs (100%)
Ethane	Methanol – water	276 – 295	Boiling, foamy slush
		296 – 304	RPTs (100 %)
		303 – 319	Popping
Propane	Water	319 – 325	Boiling, ice forms
		326 – 334	RPTs (85 %)



Cryogen	Substrate	Substrate temperature K	Result Reproducibility ¹
		335 – 356	Popping, Occasional RPTs (12%)
Propane	Ethylene Glycol	317 – 358	Boiling
Isobutane	Water	358 – 372	Boiling, Occasional popping RPTs (12 %)
Isobutane	Ethylene Glycol	298 – 348	Nucleate boiling
		352 – 377	Violent boiling
		379 – 393	Film boiling, popping
Isobutane	Ethylene Glycol – Water	370 – 373	Violent boiling
		374 – 379	RPTs (100%)
		381 – 388	Film boiling
n-butane	Water	363 – 372	Boiling, popping
Propylene	Water	303 – 312	Boiling, ice forms
		313 – 316	Popping
		317 – 346	RPTs (100%)
		347 – 363	Film boiling
Isobutylene	Ethylene Glycol	376 – 378	Eruptions
		379 – 408	RPTs (100%)

Notes: ¹. Reproducibility = 100 * Number of spills with RPT / total number of spills

Binary mixture spills on water:

Mixture	Water Temperature K	RPT range mol % of heavy component	Result Reproducibility
Ethane: Propane	293	15 – 30	75
	278	4.5 – 8	100
Ethane: n-butane	283	4.5 – 8	100
	293	2.5 – 9	100
	303	4.5 – 16	100
Ethane: n-pentane	293	2 – 9	100
Ethylene: n-butane	293	9 – 23	100
Ethylene: n-pentane	293	5 – 18	100

Peak pressures recorded were about 600 – 800 kPa (6 – 8 bars) and occurred within 4 ms from the start of an RPT. Spills were also made with mixtures containing methane and it was observed that the addition of as little as 10 mol % methane inhibited RPTs and none were ever obtained with methane concentrations in excess of 19 mol%.



Burro Series⁸

Test Setup

Eight LNG spills were performed at Naval Weapons Center, China Lake, CA in the summer of 1980.

Spill dimensions

These experiments involved 24 – 39 m³ of LNG onto water.

Instrumentation and data acquisition system

There were 25 gas stations and 5 turbulence stations arranged in arcs at 57 m, 140 m, 400 m, and 800 m from the spill point. Seven of the gas stations and one turbulence center measured humidity. In addition there were 20 wind field stations equipped with anemometers.



Table 3: Burro experiment and meteorological data summary

Test	Date (1980)	Spill vol. m ³	Spill rate m ³ /min	Avg. wind speed m/s	Spill duration sec.	Avg. wind direction Deg.	Atm. stability	Rel. humidity (avg. upstream & downstream) %	Temp. at 2-m ht. °C
Burro-2	18 Jun.	34.3	11.9	5.4	173	221	Unstable	7.1	37.6
Burro-3	2 July	34.0	12.2	5.4	167	224	Unstable	5.2	33.8
Burro-4	9 July	35.3	12.1	9.0	175	217	Slightly unstable	2.8	35.4
Burro-5	16 July	35.8	11.3	7.4	190	218	Slightly unstable	5.75	40.5
Burro-6	5 Aug.	27.5	12.8	9.1	129	220	Slightly unstable	5.0	39.2
Burro-7	27 Aug.	39.4	13.6	8.4	174	208	Neutral to slightly unstable	7.1	33.7
Burro-8	3 Sept.	28.4	16.0	1.8	107	235	Slightly stable	4.6	33.1
Burro-9	17 Sept.	24.2	18.4	5.7	79	232	Neutral	13.1	35.4

Notes: Atmospheric stability based on Richardson number.



Test Conditions

LNG composition

Test	Component (mol %)		
	Methane	Ethane	Propane
Burro-2	91.3	7.2	1.5
Burro-3	92.5	6.2	1.3
Burro-4	93.8	5.1	1.1
Burro-5	93.6	5.3	1.1
Burro-6	92.8	5.8	1.43
Burro-7	87.0	10.4	2.6
Burro-8	87.4	10.3	2.3
Burro-9	83.1	13.9	3.0

Meteorological information

Please refer to Table 3

Test Data⁹

Test	Spill plate depth (10 ⁻²) m	Pond temp.	RPT explosion	Max. Point source yield ¹ kg TNT
Burro-2	5	Greater than 17 °C	-	-
Burro-3	5		-	-
Burro-4	Below water		-	-
Burro-5	At water level		-	-
Burro-6	-		Large delayed	-
Burro-7	Above water		-	-
Burro-8	Above water		-	-
Burro-9	5 (initially)		Large early	3.5

Notes: TNT equivalence is based on the assumptions that the explosion is a point source and that the surface shock waves reflection produces an overestimate of the explosive energy by a factor of 1.8.

During the test a spill plate was located at the spill point in order to keep LNG from impinging upon and eroding the pond bottom. This plate was adjustable from a location slightly above the water surface to about 30 cm below it. No early RPTs occurred when the spill plate was located at or above the water surface while the largest RPTs occurred when the spill plate was absent.



The largest RPT observed was during the Burro-9 experiment where there was no spill plate and the spill rate was near maximum. Details of the times and magnitude of RPT explosions for Burro-9 are summarized in Table 4.

Table 4: Burro-9 RPT details⁹

Time¹	Side-on pressure²	TNT equivalence³
sec.	kPa	kg
6.5	827	0.036
7.1	1034	0.064
9.2	1861	0.295
21.4	3928	1.890
35.1	4962	3.500
43.2	689	0.023
46.0	827	0.036
54.1	827	0.036
54.9	896	0.045
66.9	1309	0.120
72.7	827	0.036

Notes: 1. $t = 0$ is start of spill valve opening.

2. Measured as a distance of 30 m

3. Equivalent free-air point-source explosion of TNT



Coyote Series¹⁰

Test Setup

The Coyote Series was conducted by Lawrence Livermore National Laboratory (LLNL) and Navy Weapons Center (NWC) in the summer and fall of 1981 at China Lake, CA, under the joint sponsorship of DOE and GRI, to investigate further Rapid Phase Transition (RPT) explosions and to determine the characteristics of fires resulting from ignition of vapor clouds of LNG spills. The series consisted of ten experiments, five emphasizing vapor cloud fires and five for investigating RPT explosions.

Spill dimensions

Coyote-1 was a small spill (14 m^3) at a rate of $6 \text{ m}^3/\text{min}$ as a result of spill malfunction. The remaining RPT spills (Coyote 4 and 8-10) consisted of three spills each. The first vapor burn experiment Coyote-2 was conducted to assess instrument capability and survivability in vapor fires. Coyote 3, 5, and 6 involved larger spills of LNG ranging from 14.6 to 28 m^3 . Coyote-7 and Coyote-8 were methane spills and Coyote-9 was performed with liquid nitrogen. In the vapor burn experiments dispersion data prior to ignition was obtained. The meteorological array and sensors were operational for Coyote-3 – 10.

Instrumentation and data acquisition system

The arrays of wind-field and gas-plus-turbulence stations are modifications of those used in the Burro series. All but six of the 31 gas and turbulence stations and five of the 20 wind field stations were located between 140 and 400 m. A total of 89 gas-concentration sensors were deployed on twenty-four gas stations and five of the six turbulence stations. LNG impact pressures and exit temperatures were measured at the spill point along with LNG composition. In addition, LNG vapor concentrations were measured at three different locations in the pond as shown in. Blast-gauges to measure RPT blast overpressures were provided at five different locations above and below the water surface and are illustrated in. No data were obtained from underwater blast gauges during any of the tests due to an electrical grounding problem.



Figure 13: Array of RPT diagnostic instrumentation¹⁰

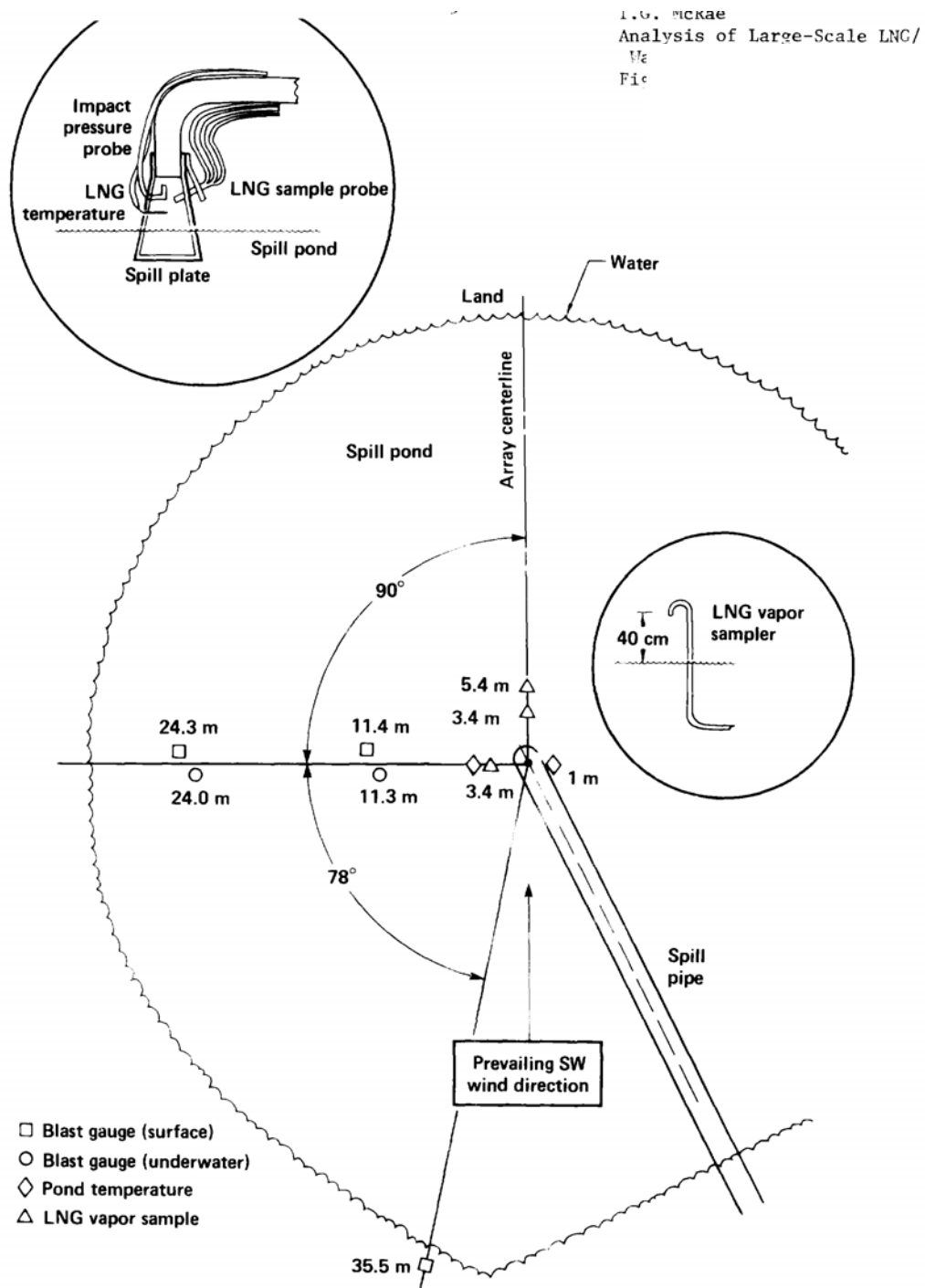




Table 5: Coyote experiment and meteorological data summary

Test	Test type	Date (1981)	Spill rate m ³ /min	Spill vol. m ³	Spill duration sec.	Avg. wind speed m/s	Avg. wind direction Deg.
Coyote-1	RPT	30 July	6	14	-	-	-
Coyote-2	Vapor burn	20 Aug.	16	8	-	-	-
Coyote-3	Vapor burn	3 Sept.	13.5	14.6	65	6	205
Coyote-4	RPT	25 Sept.	6.8	3.8	34	6.2	181
			12.1	6.0	30	6	190
			18.5	5.2	17	7.4	197
Coyote-5	Vapor burn	7 Oct.	17.1	28	98	9.7	229
Coyote-6	Vapor burn	27 Oct.	16.6	22.8	82	4.6	220
Coyote-7 ^a	Vapor burn	12 Nov.	14.0	26	111	6.0	210
Coyote-8 ^a	RPT	13 Nov.	7.5	3.7	30	8.4	206
			14.2	5.4	23	9.0	209
			19.4	9.7	30	8.5	214
Coyote-9 ^b	RPT	16 Nov.	7.2	3.6	30	2.6	158
			9.9	3.3	20	4.2	193
			13.3	8.2	37	4.2	187
Coyote-10	RPT	24 Nov.	13.8	4.6	20	7.6	223
			19.3	4.5	14	8.6	229
			18.8	5.0	16	7.2	248

Notes: a. Liquid Methane spill; b. Liquid nitrogen spill



Test Conditions

LNG composition

Test	Component (mol %)		
	Methane	Ethane	Propane
Coyote-1	-	-	-
Coyote-2	-	-	-
Coyote-3	79.4	16.4	4.2
Coyote-4	78.8	17.3	3.9
Coyote-5	74.9	20.5	4.6
Coyote-6	81.8	14.6	3.6
Coyote-7	99.5	0.5	-
Coyote-8	99.7	0.3	-
Coyote-9	-	-	-
Coyote-10	70.2	17.2	12.6

Test Data

Test	Spill plate depth (10 ⁻²)		Impact pressure (kPa)		Pond temp. °C	RPT explosions	Max. point source yield
	m		Max.	Avg.			kg TNT
Coyote-1	30		5.5	1.4	30	Small early Large delayed	-
Coyote-2	2.5		34.5	34.5	27.6	Small early	0.23
Coyote-3	2.5		68.9	41.3	22.8	-	-
Coyote-4	a.	25	16.5	2.8	22.4	Small early	0.001
	b.	25	34.5	20.7	20.6	-	-
	c.	25	68.9	34.5	20.2	Large early	1.5
Coyote-5	6		89.6	55.1	17.2	Large delayed	3.0
Coyote-6	5		89.6	55.1	15	-	-
Coyote-7	33		103.4	41.3	13.6	-	-
Coyote-8	a.	33	13.8	4.1	12.8	-	-
	b.	33	68.9	27.6	12.7	-	-
	c.	33	96.5	75.8	12.3	-	-
Coyote-9	a.	36	13.8	1.4	14.1	-	-
	b.	36	55.1	20.7	14.8	-	-
	c.	36	103.4	68.9	15.8	-	-
Coyote-10	a.	36	55.1	34.5	10.6	-	-
	b.	36	96.5	68.9	10.6	-	-
	c.	removed	82.7	62.0	11.6	Small early	0.005

RPT yield correlates favorably with spill rate. The data indicates an apparent threshold or abrupt increase in the RPT explosive yield at a spill rate of about 15 m³/min.⁹ For large scale spills large RPTs can occur for initial methane composition as high as 90%.⁹



Falcon Series¹¹

Test Setup

A series of five LNG spills on water up to 66 m³ in volume were performed within a vapor barrier structure at Frenchman Flat on Nevada Test Site by Lawrence Livermore National Laboratory (LLNL) for the Department of Transportation (DOT) and the Gas Research Institute (GRI) in the summer of 1987. These tests were performed to evaluate the effectiveness of vapor fences as a mitigation technique for accidental release of LNG.

Spill dimensions

Test	Date	Spill rate	Spill vol.	Spill duration
	(1987)	m ³ /min	m ³	sec.
Falcon-1	12 June	28.7	66.4	138.8
Falcon-2	18 June	15.9	20.6	77.7
Falcon-3	29 June	18.9	50.7	160.9
Falcon-4	21 Aug.	8.7	44.9	309.7
Falcon-5	29 Aug.	30.3	43.9	86.9

Instrumentation and data acquisition system

A barrier was placed upwind of the pond inside the fence to generate turbulence typical of a storage tank. Gas concentration, wind field, turbulence, temperature, heat flux, humidity, and air pressure were measured during each experiment.

Test Conditions

LNG composition

Test	Component (mol%)	
	Methane	Heavies
Falcon-1	94.7	3.9
Falcon-2	95.6	3.7
Falcon-3	91.0	8.0
Falcon-4	91.0	8.0
Falcon-5	88	10



Meteorological information

Test	Avg. wind speed at 2-m ht. m/s	Avg. wind direction at 2-m ht Deg.	Rel. humidity %	Stability class
Falcon-1	1.7	5.46	-	G
Falcon-2	4.7	8.27	-	D
Falcon-3	4.1	8.41	4	D
Falcon-4	5.2	5.82	12	D/E
Falcon-5	2.8	7.70	13.7	E/F

Test Data¹²

Test	Notes
Falcon-1	Significant overfilling of vapor barrier structure causing excessive spilling early in the test
Falcon-2	-
Falcon-3	-
Falcon-4	RPT explosions started at 60 s
Falcon-5	RPT explosions started at 60 s. Fire started at 81 s



References

- ¹. Nakanishi, E., and Reid, R.C., "Liquid Natural Gas - Water Reactions", Chem. Engg. Progress, Vol. 67 (12), 36 - 41, Dec. 1971
- ². Burgess, D., Biordi, J., and Murphy, J., "Hazards of Spillage of LNG into Water", U.S. Dept. of the Interior, Bureau of Mines, Pittsburgh, PMSRC report no. 4177, 1972.
- ³. Garland, F., and Atkinson, G., "The Interaction of Liquid Hydrocarbons with Water", Rpt. No. AD-753561, US DOT, USCG, Oct. 1971.
- ⁴. Enger, T. "Explosive Boiling of Liquefied Gases on Water", Proceeding of the conf. on LNG import and terminal safety, Boston, 1972.
- ⁵. Feldbauer, G.F., Heigl, J.J., McQueen, W., Whipp, R.H., and May, W.G., "Spills of LNG on Water: Vaporization and Downwind Drift of Combustible mixtures", ESSO Research and Engg. Co., Report no. EE61E-72, 1972.
- ⁶. Gas Research Institute, "MIT-GRI LNG Safety and Research Workshop, Vol .1 RPT", GRI 82/0019.1, Aug. 1982.
- ⁷. Porteous, W. M., and Reid, R.C., "Light Hydrocarbon Vapor Explosions on Water", LNG Research Center, MIT, Dec. 1972.
- ⁸. Koopman, R.P., Baker, J., Cederwall, R.T., Goldwire, Jr., H.C., Hogan, W.J., Kamppinen, L.M., Keifer, R.D., McClure, J.W., McRae, T.G., Morgan, D.L., Morris, L.K., Spann, Jr., M.W., Lind, C.D., "Burro Series Data Report. LLNL/NWC 1980 LNG Spill Test", UCID 19075, Dec. 1982.
- ⁹. McRae, T.G., Goldwire, Jr., H.C., and Koopman, R.P., "Analysis of Large-Scale LNG/Water RPT Explosions", Lawrence Livermore National Laboratory, UCRL-91832, Oct. 1984.
- ¹⁰. Goldwire, Jr., H.C., Rodean, H.C., Cederwall, R.T., Kansa, E.J., Koopman, R.P., McClure, J.W., McRae, T.G., Morris, L.K., Kamppinen, L., Kiefer, R.D., Urtview, P.A., "Coyote Series Data Report. LLNL/NWC 1981 LNG Spill Test Dispersion, Vapor Burn, and Rapid-Phase-Transition.", UCID-19953, Vol. 1, 2, Oct. 1983.
- ¹¹. Brown, T.C., Cederwall, R.T., Chan, S.T., Ermak, D.L., Koopman, R.P., Lamson, K.C., McClure, J.W., and Morris, L.K., "Falcon Series Data Report 1987 LNG Vapor Barrier Verification Field Trials", Tech. report GRI-89/0138,LLNL, Feb. 1990.
- ¹². Melhem, G.A., "LNG Release Assessment", Arthur D. Little, Final Report to the US DOT, Ref. 61230-30, Feb. 1991.